



Oceanic microplate formation records the onset of India–Eurasia collision



Kara J. Matthews^{a,*}, R. Dietmar Müller^a, David T. Sandwell^b

^a EarthByte Group, School of Geosciences, The University of Sydney, Sydney, NSW 2006, Australia

^b Scripps Institution of Oceanography, La Jolla, CA 92093, USA

ARTICLE INFO

Article history:

Received 17 September 2015

Received in revised form 22 October 2015

Accepted 22 October 2015

Available online 4 November 2015

Editor: A. Yin

Keywords:

microplate

extinct ridge

pseudofault

Indian Ocean

India–Eurasia collision

plate reorganization

ABSTRACT

Mapping of seafloor tectonic fabric in the Indian Ocean, using high-resolution satellite-derived vertical gravity gradient data, reveals an extinct Pacific-style oceanic microplate ('Mammerickx Microplate') west of the Ninetyeast Ridge. It is one of the first Pacific-style microplates to be mapped outside the Pacific basin, suggesting that geophysical conditions during formation probably resembled those that have dominated at eastern Pacific ridges. The microplate formed at the Indian–Antarctic ridge and is bordered by an extinct ridge in the north and pseudofault in the south, whose conjugate is located north of the Kerguelen Plateau. Independent microplate rotation is indicated by asymmetric pseudofaults and rotated abyssal hill fabric, also seen in multibeam data. Magnetic anomaly picks and age estimates calculated from published spreading rates suggest formation during chron 21o (~47.3 Ma). Plate reorganizations can trigger ridge propagation and microplate development, and we propose that Mammerickx Microplate formation is linked with the India–Eurasia collision (initial 'soft' collision). The collision altered the stress regime at the Indian–Antarctic ridge, leading to a change in segmentation and ridge propagation from an establishing transform. Fast Indian–Antarctic spreading that preceded microplate formation, and Kerguelen Plume activity, may have facilitated ridge propagation via the production of thin and weak lithosphere; however both factors had been present for tens of millions of years and are therefore unlikely to have triggered the event. Prior to the collision, the combination of fast spreading and plume activity was responsible for the production of a wide region of undulate seafloor to the north of the extinct ridge and 'W' shaped lineations that record back and forth ridge propagation. Microplate formation provides a precise means of dating the onset of the India–Eurasia collision, and is completely independent of and complementary to timing constraints derived from continental geology or convergence histories.

© 2015 Elsevier B.V. All rights reserved.

1. Introduction

Satellite gravity data have been used for decades to map major tectonic structures on the seafloor, on a near-global scale (e.g. Matthews et al., 2011; De Alteriis et al., 1998; Gahagan et al., 1988). In particular, fracture zones, active and extinct ridges and pseudofaults can produce strong gravity signals making them ideal mapping targets. A recent satellite altimetry-derived vertical gravity gradient (VGG) dataset (Sandwell et al., 2014) resolves structures as small as 6 km in width, enabling improved mapping of seafloor structures compared to previous versions. Increased resolution not only reveals new seafloor structures, but also confirms the existence of structures previously identified with lower confi-

dence, which can then be used to improve plate kinematic models and constrain the timing of plate boundary reorganizations.

VGG mapping in Eocene seafloor in the eastern Indian Ocean has revealed a number of distinctive tectonic lineations that are datable using magnetic anomaly picks. Specifically we have identified possible extinct Indian–Antarctic ridge segments, conjugate pseudofaults and an oceanic microplate that underwent independent rotation (Fig. 1a). The significance of these structures is two-fold. Not only is this the first time a Pacific-style microplate has been identified in the Indian Ocean, suggesting geophysical conditions at the Indian–Antarctic ridge probably resembled those that have dominated at Pacific ridges, however the formation of these structures also coincides with, and we argue is linked to the history of the India–Eurasia collision – the time of which is a major and long-standing controversy in plate tectonics. Microplate formation as a means of dating the India–Eurasia collision is completely

* Corresponding author.

E-mail address: kara.matthews@sydney.edu.au (K.J. Matthews).

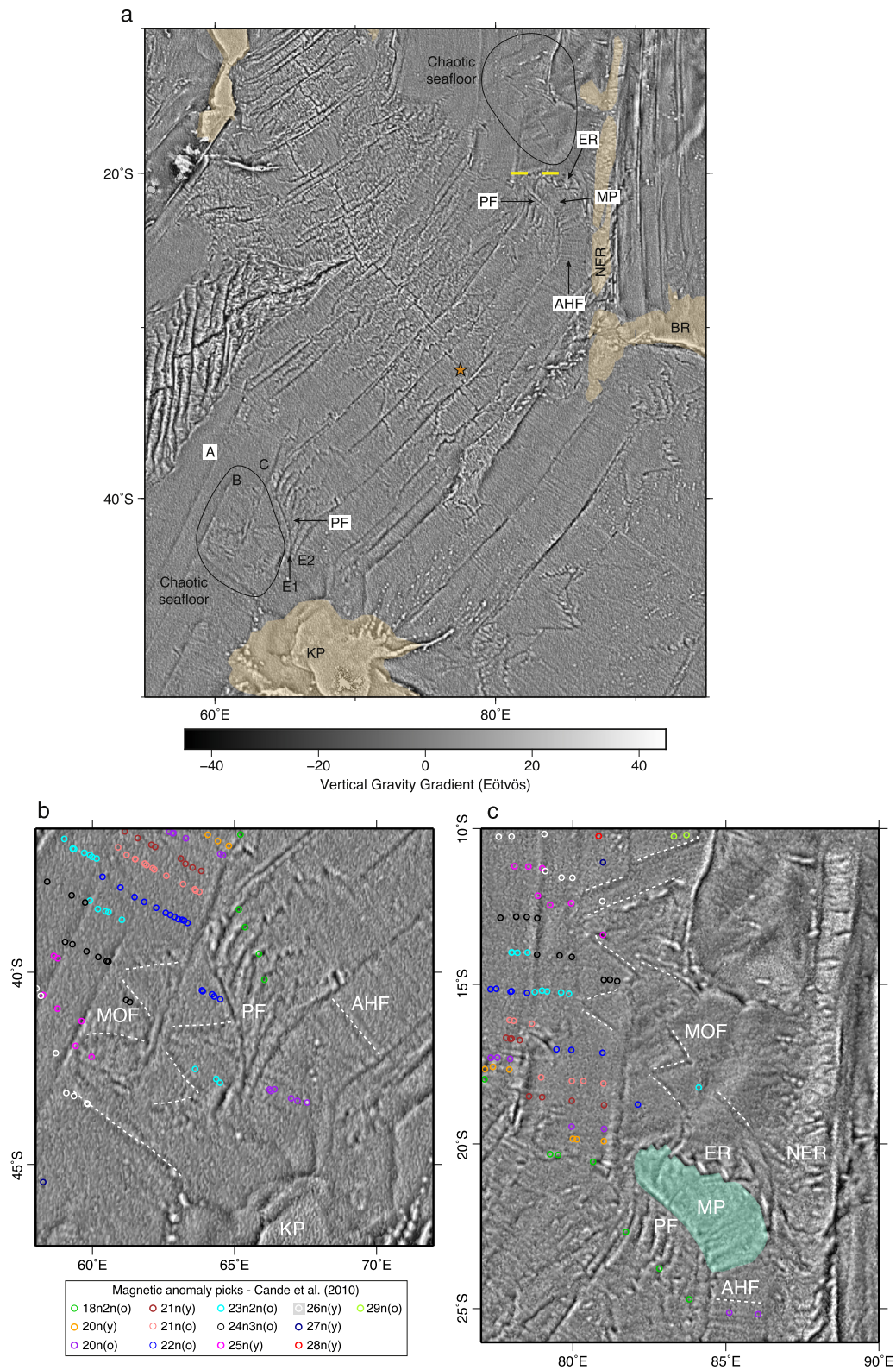


Fig. 1. VGG maps (Sandwell et al., 2014) of the eastern/southeastern Indian Ocean basin, showing key seafloor structures that were mapped using the VGG data and described in Section 4. These include two pseudofaults (PF), an extinct ridge (ER), a microplate (MP) – the ‘Mammerickx Microplate’ (see Section 5), abyssal hill fabric (AHF), and ‘migrating offset fabric’ (MOF) comprising ‘W’ shaped lineations produced by back and forth ridge propagation. Several fracture zones are also labeled A, B, C, E1 and E2 (also shown in Fig. 3). (a) Regional map with large igneous provinces (from Whittaker et al., 2015) shown in transparent yellow, and the ship track segments from Fig. 5 in yellow (Sojourn Expedition Leg 4, R/V Melville, 1997). An orange star identifies the location at the Southeast Indian Ridge where spreading rates were calculated using the Euler rotation poles of Cande and Patriat (2015). (b)–(c) Zoomed in maps of the Antarctic Plate north of the Kerguelen Plateau (KP), and the Indian Plate west of the Ninetyeast Ridge (NER), respectively, showing magnetic anomaly picks of Cande et al. (2010). Traces of the seafloor lineations produced by back and forth ridge propagation (dashed white lines), that make up the ‘chaotic seafloor’ from a, are offset from their negative gravity anomalies so as not to obscure their signal. The Mammerickx Microplate is shaded green. BR, Broken Ridge. (For interpretation of the references to color in this figure legend, the reader is referred to the web version of this article.)

independent to those timing constraints derived from continental geology or the India–Eurasia convergence history.

1.1. India–Eurasia collision and its seafloor record

One of the most intensively studied and strongly debated issues in plate tectonics is the timing and nature of the India–Eurasia collision. This event marked the closure of the NeoTethys Ocean basin, the youngest and final of the Tethyan oceans that separated Gondwana from Asia since the Paleozoic, and moreover it led to the rise of the Himalayas, the highest mountain chain on Earth. Proposed timings of the India–Eurasia collision vary by more than 30 Myr (e.g. [Patriat and Achache, 1984](#); [Searle et al., 1987](#); [Klootwijk et al., 1992](#); [Lee and Lawver, 1995](#); [Rowley, 1998](#); [Aitchison et al., 2007](#); [van Hinsbergen et al., 2012](#); [Zahirovic et al., 2012](#); [Bouilhol et al., 2013](#); [Gibbons et al., 2015](#)), and there is debate over whether there was a single continent–continent collision event (e.g. [Patriat and Achache, 1984](#); [Lee and Lawver, 1995](#)) or multiple collisions, with India first colliding with an island arc and later with Eurasia (e.g. [Aitchison et al., 2007](#); [Zahirovic et al., 2012](#); [Bouilhol et al., 2013](#)), or with a microcontinent–Eurasia collision followed by the India–Eurasia collision ([van Hinsbergen et al., 2012](#)).

Different observations have been used to constrain the timing and nature of the event, including changes in sedimentation patterns – such as the cessation of marine sedimentation in the suture zone and the beginning of continental molasse sedimentation (e.g. [Searle et al., 1987](#); [Aitchison et al., 2007](#)), arc magmatic records – for instance the ending of calc-alkaline magmatism (e.g. [Bouilhol et al., 2013](#)), the decrease in India–Asia convergence inferred from magnetic lineations in the Indian Ocean ([Molnar and Taponnier, 1975](#); [Patriat and Achache, 1984](#); [Lee and Lawver, 1995](#)), basin subsidence patterns ([Rowley, 1998](#)), paleomagnetic data from the Indian Plate and Himalayan region ([Klootwijk et al., 1992](#)), and the analysis of the mantle structure beneath the Tethyan region as inferred from seismic tomography models ([van der Voo et al., 1999](#); [Replumaz et al., 2004](#); [Hafkenscheid et al., 2006](#)). Additionally, global mantle convection modeling combined with seismic tomography analysis has enabled the testing of existing end-member kinematic models ([Zahirovic et al., 2012](#)). There is growing support for a complex multiple collision model in which India collided with an island-arc that was outboard of Asia at ~55–50 Ma, the Kohistan–Ladakh Arc, and then final India–Eurasia collision occurred closer to 40 or 30 Ma (e.g. [Hafkenscheid et al., 2006](#); [Aitchison et al., 2007](#); [Zahirovic et al., 2012](#); [Bouilhol et al., 2013](#); [Gibbons et al., 2015](#)) and was likely diachronous (e.g. [Zahirovic et al., 2012](#)). Furthermore the collision of India with Eurasia may be more accurately defined as a protracted event that included a ‘soft’ collision phase followed by a ‘hard’ collision phase (e.g. [Gibbons et al., 2015](#)).

Recently, [Cande and Patriat \(2015\)](#) suggested that the slowdown of India around chron 21o (47.3 Ma), which is sharper using the GTS12 timescale ([Ogg, 2012](#)) than in previous timescales, is consistent with the initial India–Eurasia collision. However, they noted some ambiguity in this timing considering that the sharp change in azimuth of seafloor spreading between the Capricorn and African plates does not occur until after chron 20o (43.4 Ma). This ambiguity is also reflected in a recent review of the India–Eurasia collision using a synthesis of a range of marine geophysical and continental geological observations by [Gibbons et al. \(2015\)](#), who proposed that India collided with an intraoceanic arc at ~52 Ma (arc–continent collision), followed by an initial soft collision of India with Eurasia (continent–continent collision) around 44 ± 2 Ma.

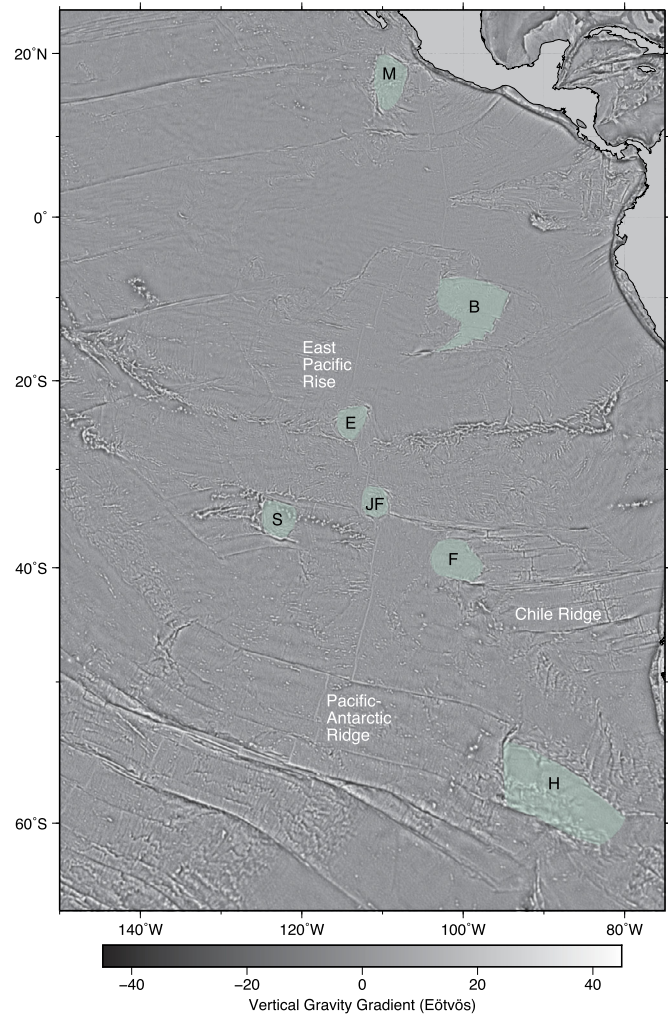


Fig. 2. VGG map ([Sandwell et al., 2014](#)) of the eastern Pacific Ocean basin, showing active and extinct microplates (transparent green). The Pacific–Antarctic Ridge and East Pacific Rise produce positive VGG anomalies, while the Chile Ridge produces a negative VGG anomaly. B, Bauer Microplate (extinct); E, Easter Microplate (active); F, Friday Microplate (extinct); H, Hudson Microplate (extinct); JF, Juan Fernandez Microplate (active); M, Mathematician Microplate (extinct); S, Selkirk Microplate (extinct). (For interpretation of the references to color in this figure legend, the reader is referred to the web version of this article.)

2. Oceanic microplates

During spreading ridge reorganizations sections of oceanic crust can be transferred from one plate to another due to instantaneous ridge jumps (e.g. [Small, 1995](#)) or ridge propagation into existing seafloor ([Hey, 1977](#)), resulting in asymmetric lithosphere accretion. In the latter case, the captured rigid blocks are commonly referred to as microplates (also ‘paleoplates’). Microplates are rigid bodies between two active spreading ridges that rotate approximately independently of neighboring plates ([Mammerickx and Klitgord, 1982](#)). Spreading dwindles and then ceases at one of the ridges, leading to detachment of the microplate from the spreading axis and transfer to one of the major plates. The microplate consists of both the captured lithosphere, and the lithosphere that accreted during dual spreading ([Mammerickx and Klitgord, 1982](#)). [Tebbens et al. \(1997\)](#) expanded the definition of [Mammerickx and Klitgord \(1982\)](#) to include microplate formation in the absence of ridge death. This was based on their discovery of the Friday Microplate in the southeastern Pacific, ~500 km west of the Chile Ridge ([Fig. 2](#)). According to [Tebbens et al. \(1997\)](#) the Friday Microplate formed from the step-wise migration of the Pacific–

Nazca–Antarctic triple junction at chron 5A (~12 Ma). The Chile Ridge (Nazca–Antarctic spreading arm of the triple junction) propagated into the Nazca Plate, whereby isolating a section of Nazca crust. Asymmetry in the shape of the associated Friday and Crusoe pseudofaults confirms there was independent rotation of the Friday Microplate during formation (Tebbens et al., 1997).

Microplate formation and ridge propagation have been intensively studied in the Pacific for more than 40 years (e.g. Hey, 1977; Hey et al., 1980, 1988; Hey and Wilson, 1982; Mammerickx et al., 1988; Schouten et al., 1993; Searle et al., 1993; Bird and Naar, 1994; Tebbens et al., 1997; Tebbens and Cande, 1997; Blais et al., 2002; Eakins, 2002; Eakins and Lonsdale, 2003). Here there are several actively forming microplates (e.g. Easter, Juan Fernandez, Galapagos) and detached Cenozoic ones (e.g. Mathematician, Bauer, Friday, Selkirk, Hudson) (Fig. 2).

Building on the work of Schouten et al. (1993), both Bird and Naar (1994) and Eakins (2002) emphasized that plate reorganizations are a trigger for changing the coupling at free-slip boundaries, that can result in tearing of one or both plates and the initiation of a propagator from a ridge spreading offset (see summary of Hey, 2004). As the propagator grows the microplate core rotates due to the drag of the adjacent plates. Both transpression or transtension-inducing plate motion changes can increase shear coupling across a previously free-slipping boundary (Bird and Naar, 1994; Eakins, 2002).

In addition to plate motion changes, hotspot activity and fast seafloor spreading can drive or facilitate ridge propagation and microplate formation, as they contribute to stress changes at the ridge and production of regions of hot, thin or weakened lithosphere that is able to concentrate stress (e.g. Hey et al., 1985; Bird and Naar, 1994; Hey, 2004). Furthermore, hotspot activity also produces elevated topography which is a driver of ridge propagation, with ridge propagation directed away from hotspots (Phipps Morgan and Parmentier, 1985). Microplate formation can also occur during step-wise triple junction migration (Tebbens et al., 1997; Tebbens and Cande, 1997; Bird et al., 1999).

Microplate rotation produces ‘oblique seafloor’ rather than typical ridge parallel and perpendicular structures (Hey, 2004). A fan shaped pattern of isochrons and rotated abyssal hills are characteristic features (Hey et al., 1988; Mammerickx et al., 1988; Eakins, 2002; Hey, 2004). Ridge propagation produces a pair of pseudofaults across which young lithosphere formed at the new ridge is juxtaposed against older lithosphere. These lineations, defining seafloor age contrasts, are commonly identifiable as negative gravity anomalies. Pseudofault pairs are often near mirror images of each other, although microplate rotation can reduce this symmetry (Tebbens et al., 1997). If spreading ceases at one of the microplate boundaries, signaling an end to dual spreading, then an extinct ridge may also be identifiable in the seafloor fabric, as is adjacent to the Mathematician, Hudson, Selkirk and Bauer microplates.

3. Methodology

The VGG dataset of Sandwell et al. (2014) is used to map seafloor fabric in the eastern and southern Indian Ocean, specifically structures that formed at the Southeast Indian Ridge from spreading between India and Antarctica. Compared to free-air gravity, VGG data better resolve short wavelength structures such as fracture zones. By combining new altimeter measurements from the CryoSat-2 and Jason-1 satellites with older data from Geosat and ERS-1 the Sandwell et al. (2014) VGG dataset provides unprecedented resolution and resolves structures as small as 6 km in width. It therefore provides a unique opportunity to improve seafloor mapping and confirm or identify new tectonic structures that can constrain plate tectonic models. Multibeam ship track data

collected during the Sojourn Expedition Leg 4, R/V Melville, 1997, were also used during mapping (Fig. 1) (NOAA National Centers for Environmental Information, 2004).

Structures identified in the VGG maps are dated using magnetic anomaly picks where possible. The primary source of magnetic anomaly picks in our regions of interest is Cande et al. (2010). Several magnetic anomaly picks from Ségoufin et al. (2004) are also used to supplement those from Cande et al. (2010). The GTS2012 timescale of Ogg (2012) is adopted, and a ‘y’ or ‘o’ is used to describe whether the young or old end of the magnetic chron was picked, respectively. Absolute seafloor ages are supplemented with seafloor ages derived from relative dating. Relative age dating helps clarify the sequence of tectonic events in the absence of tight absolute age constraints, and can provide valuable estimates on the minimum and maximum ages of structures. Cande and Patriat (2015) provide finite Euler rotation poles for spreading between India and Antarctica and we have used these data, in conjunction with the open-source plate reconstruction software *GPlates* (Boyden et al., 2011) to calculate spreading rates at the Southeast Indian Ridge, specifically at the point shown in Fig. 1. These spreading rates allow us to estimate seafloor ages where magnetic anomaly picks are absent.

4. Eocene seafloor tectonic fabric of the eastern and southern Indian Ocean

In the eastern Indian Ocean a >500 km long E–W to NW–SE trending structure that resembles an extinct spreading ridge is located at ~21.5°S, to the west of the Ninetyeast Ridge (Figs. 1 and 3). It has a step-like pattern that mainly comprises segments 30–70 km in length with a negative VGG signature, although some segments comprise a positive VGG signature. The structure curves southwards in the east, along the western edge of the Ninetyeast Ridge.

To the south of the eastern part of the extinct ridge-like structure abyssal hill fabric is discernable in VGG maps (Figs. 1 and 3). Near the chron 20o (43.4 Ma) magnetic anomaly picks of Cande et al. (2010) the abyssal hill lineations are oriented ~97° (Fig. 1c). As abyssal hills form roughly perpendicular to the direction of seafloor spreading, their orientation indicates that the direction of spreading was approximately N–S and that this seafloor formed prior to the major clockwise change in spreading direction at the ridge that occurred at chron 20 according to Cande et al. (2010). The abyssal hills north of this appear to have been rotated counterclockwise by 25°. Their orientation is not perpendicular to the direction of spreading that preceded (~N–S), nor post-dated (~SSW–NNE), the chron 20 spreading reorganization at the Southeast Indian Ridge, suggesting that the crust was rotated after formation (Fig. 3).

Lying 100–200 km to the south of the extinct ridge-like feature is a NW–SE trending linear structure, ~350 km in length and characterized by a VGG low (Figs. 1 and 3). A comparable structure (trending NNW–SSE) is also observed on the Antarctic Plate in the same spreading corridor, north of the Kerguelen Plateau (Figs. 1 and 3). Their VGG widths (~10 km) are similar to, or slightly smaller than adjacent fracture zones. These structures, however, are oblique to adjacent fracture zones and nearly orthogonal to fracture zones formed in younger crust, and therefore are not fracture zones despite having a similar gravity signature. At their eastern ends they emanate from the same location as fracture zones E1–2 (Fig. 3) that continue in younger crust and can be traced to the present-day spreading ridge. These structures are also a divide between a highly segmented spreading system with closely spaced fracture zones (younger crust), and a spreading system with widely spaced fracture zones and ‘W’ shaped lineations produced by the migration of non-transform ridge offsets (older crust).

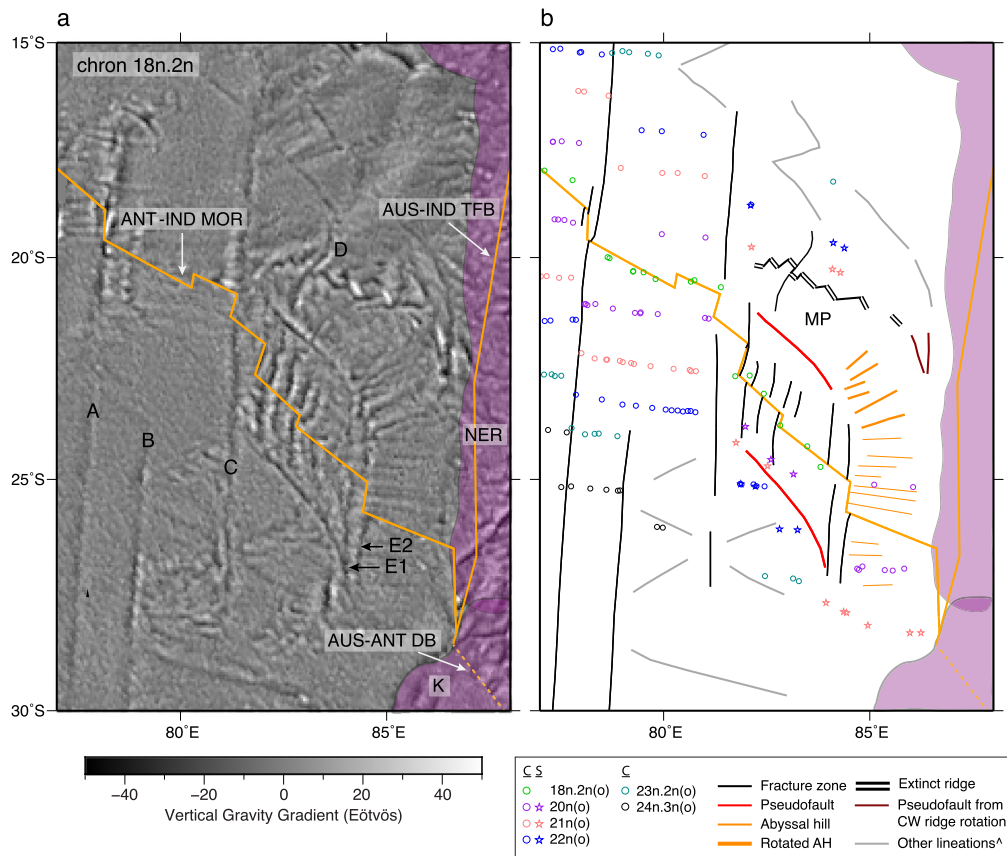


Fig. 3. A chron 18n.2n (40.1 Ma) reconstruction, in an India-fixed reference frame, of (a) the VGG data (Sandwell et al., 2014), and (b) the magnetic anomaly picks and tectonic fabric traces. The plate reconstruction software *GPlates* (Boyden et al., 2011) was used to reconstruct the data using the Seton et al. (2012) global plate reconstruction model. Magnetic anomaly picks are from Cande et al. (2010) (circles) and Ségoufin et al. (2004) (stars). Fracture zone traces are from Matthews et al. (2011). Plate boundaries are continuous dark orange lines; the Australian–Antarctic plate boundary is represented by a dashed line as it may have been a diffuse boundary at this time (Whittaker et al., 2013). Spreading (white on black lines) and transform (solid black lines) segments of the extinct ridge have been distinguished from the VGG data. Several key fracture zones are labeled A–E2 in (a). ANT–IND MOR, Antarctic–Indian mid-ocean ridge; AUS–ANT DB, Australian–Antarctic diffuse boundary; AUS–IND TFB, Australian–Indian transform boundary; K, Kerguelen Plateau; NER, Ninetyeast Ridge; MP, microplate. (For interpretation of the references to color in this figure legend, the reader is referred to the web version of this article.)

On the Indian Plate, to the north of the proposed extinct ridge, there is a zone of chaotic seafloor fabric devoid of fracture zone traces (Fig. 1a), unlike what has previously been identified from free-air gravity (Krishna et al., 2012). Here distinctive ‘W’ shaped lineations (oblique to the direction of spreading) record the migration of small ridge offsets, that is, back and forth ridge propagation similar to what is described by Phipps-Morgan and Sandwell (1994) along the Southeast Indian Ridge (Fig. 1c). The formation of these features reveals the absence of a stable transform fault at the spreading ridge that is required for the formation of fracture zones. This type of seafloor fabric is also seen on the Antarctic Plate (Fig. 1b) between fracture zones B and C, and C and E (Fig. 3). Additionally, on the Indian Plate in this region of chaotic seafloor fabric the seafloor appears undulate, in contrast to the relatively flat seafloor seen to the west of fracture zone C away from this zone (Fig. 4), likely related to Kerguelen Plume activity.

A comparison of seafloor fabric on the Indian and Antarctic plates reveals regions of symmetry and asymmetry, with seafloor fabric symmetry expected from a simple spreading history. To the east of the fracture zone C on both plates (Fig. 3) there is a distinctive asymmetry in the seafloor fabric (from at least chron 29o, Fig. 1b–c) that supports previous suggestions of ridge jumps and asymmetric crustal accretion (e.g. Krishna et al., 1995). To the west of fracture zone C (in the spreading corridors between fracture zones A–B and B–C, Fig. 3) the seafloor fabric is largely symmetric, with features on one plate mirrored on the other plate. For instance, a set of distinctive ‘W’ shaped lineations on the Indian Plate

(seafloor older than chron 22o), which are oblique to the fracture zones, are also seen on the Antarctic Plate, although here their signal is slightly weaker. These pseudofault and extinct ridge traces are produced during short-lived ridge propagation events that have been widely observed at the Southeast Indian Ridge (Phipps-Morgan and Sandwell, 1994).

4.1. Tectonic fabric interpretations

The tectonic fabric features described above are most likely a result of ridge extinction, microplate formation and rotation, and a ridge jump involving ridge propagation. In particular they share a strong resemblance to well-studied structures produced by microplate formation, ridge extinction and ridge propagation in the eastern Pacific.

The pattern seen in the VGG maps created by the proposed extinct ridge, particularly its segmentation, is very similar to that of currently active mid-ocean ridges. Considering that this structure also largely trends perpendicular to the direction of spreading between the Indian and Antarctic plates during the Eocene, in a region of previously identified ridge jumps, we interpret this feature as an extinct spreading ridge. The scale of segmentation observed is similar to that of the present-day central Mid-Atlantic and Central Indian ridges, and is consistent with a slow-intermediate spreading regime with half-spreading rates less than 30 mm/yr (Sandwell and Smith, 2009). This is much slower than the spreading rate during creation of older crust in the region, to the north

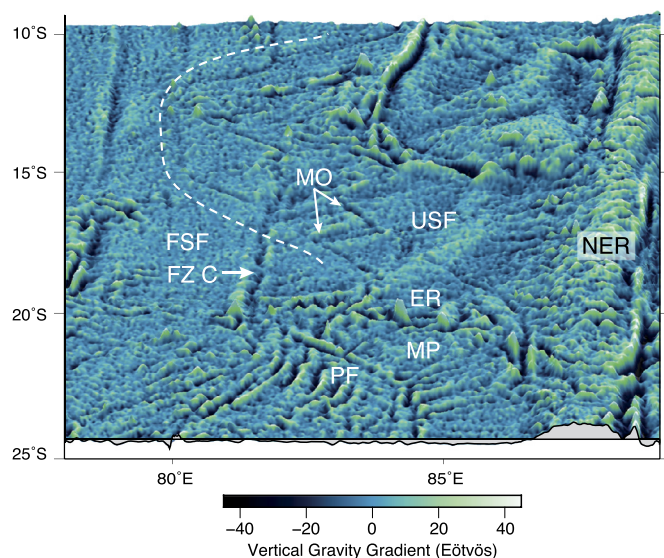


Fig. 4. 3-D perspective VGG map of the microplate and region of chaotic seafloor to the north, draped over the SRTM30 Plus V11.0 digital elevation model (Becker et al., 2009). Along the southern map boundary a horizontal plane has been inserted at 4 km depth. The white dashed line separates chaotic undulate seafloor in the east (to the north of the microplate and west of the Ninetyeast Ridge, NER), from relatively flat seafloor immediately to the west. Fracture zones are also largely absent from the seafloor to the east of the dashed line, rather 'W' shaped lineations produced by migrating spreading ridge offsets (MO) are dominant. ER, extinct ridge; FSF, flat seafloor; FZ C, fracture zone C (see Figs. 1a and 3); MP, microplate; PF, pseudofault; USF, undulate seafloor.

of the extinct ridge, which exceeded 50–60 mm/yr (half-rate) during the latest Cretaceous and Paleocene (Seton et al., 2012; Cande and Patriat, 2015). An increase in roughness adjacent to the ridge, compared to older seafloor, and increased ridge segmentation likely reflect a decrease in spreading rate, which can occur during the demise of a ridge prior to extinction (Livermore et al., 2000).

The curvature of this structure in the east adds further support to its classification as an extinct ridge. Curvature and migration of a dying spreading ridge have been observed in the Pacific associated with formation of the Bauer and Selkirk microplates (Eakins and Lonsdale, 2003; Blais et al., 2002). In these scenarios migration of the dying ridges occurred during dual-spreading and in both instances migration was towards the new ridge and microplate core. At the Bauer Microplate the Galapagos Rise grew in a southwestward direction during clockwise rotation, and in response the seafloor rotated in a counterclockwise direction to the north of the Atahualpa Scarp and west of the propagating ridge. Specifically there was a $\sim 25^\circ$ counterclockwise rotation of pre-existing seafloor which is observed in abyssal hill trends identified from multibeam bathymetry data (Eakins and Lonsdale, 2003, e.g. Fig. 3, p. 174). Similarly to the Bauer Microplate, a 25° counterclockwise rotation of abyssal hill fabric is also identified to the south of the eastern Indian Ocean proposed extinct ridge, adjacent to where the ridge curves southward (Figs. 1 and 3). This suggests that southward growth of the ridge prior to extinction disrupted pre-existing seafloor fabric.

Rotation of the dying ridge is also demonstrated by the curvature of what is interpreted to be a fracture zone that formed at the ridge (Fig. 3, fracture zone D). The northern fracture zone strand curves to the east, while the southern fracture zone strand curves to the west. The asymmetry seen between the northern and southern strands is consistent with a rotating ridge, as if there was migration of a transform offset during spreading, which also produces structures oblique to the direction of spreading, then the resultant seafloor traces would be symmetric across the ridge. Near

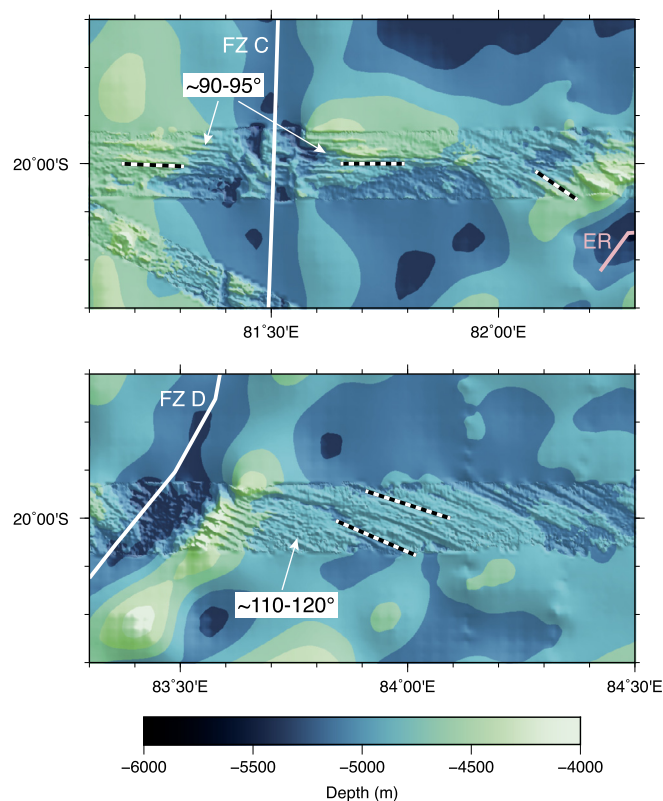


Fig. 5. Multibeam bathymetry (Sojourn Expedition Leg 4, R/V Melville, 1997) collected north of the identified extinct ridge (ER), highlighting changes in the orientation of abyssal hills (see Fig. 1 for location). Black and white lines indicate the orientation of the abyssal hills. Adjacent to fracture zone C (FZ C) they are oriented $\sim 90\text{--}95^\circ$ (a), while adjacent to fracture zone D (FZ D) (b) and closer to the extinct ridge trace (a) they are oriented $\sim 110\text{--}120^\circ$.

this fracture zone abyssal hill fabric is identified from ship track multibeam bathymetry (Sojourn Expedition Leg 4, R/V Melville, 1997) (Fig. 5). The abyssal hills have an azimuth of $\sim 110\text{--}120^\circ$ to the east of fracture zone D, while directly to the east and west of fracture zone C they have an azimuth of $\sim 90\text{--}95^\circ$, which is perpendicular to the direction of spreading between the Indian and Antarctic plates.

The very distinctive linear, 350 km long NW–SE and NNW–SSE trending gravity lows on the Indian and Antarctic plates, respectively, are interpreted to be conjugate features. We interpret these as pseudofaults of a new, westward propagating ridge that succeeded the extinct ridge. The pseudofaults are slightly asymmetric indicating independent motion of the microplate and their low angle with respect to the pre-existing and newly established ridge indicates fast propagation. The pseudofaults are to the south of the extinct ridge indicating that the plate boundary reorganization involved a southward ridge jump. Pseudofault pairs are common and distinctive seafloor structures across which there is an age contrast yet no relative motion (hence 'pseudo'), such as the Pacific Friday and Crusoe troughs (Chile Ridge, e.g. Tebbens et al., 1997), the Henry and Hudson troughs (Pacific–Antarctic ridge, e.g. Tebbens and Cande, 1997) and the Moctezuma and Michoaca troughs (near the Mathematician Microplate, e.g. Mammerickx et al., 1988). These eastern and southern Indian Ocean pseudofaults produce a similarly distinctive gravity signal.

The ridge propagation event was accompanied by the establishment of well-defined transform faults at the origin of propagation, and this is seen in the fracture zone patterns. Fracture zones E1–2 (Fig. 3) initiate at the time of propagation and are absent in older crust. Fracture zones form from stable transform fault ridge offsets

that are typically greater than 30 km (MacDonald et al., 1991), and therefore the establishment of fracture zones E1–2 suggests that the offset at the mid-ocean ridge from which the propagating ridge spawned was small and subsequently grew.

4.2. Temporal constraints

Magnetic anomaly picks help constrain seafloor ages in these regions of the Indian Ocean where we have identified a pseudofault pair and extinct ridge (Cande et al., 2010; Ségoufin et al., 2004). They are more densely distributed in the spreading corridor to the west of fracture zone C, compared to the spreading corridors to the east (Fig. 3). However, some key picks near the extinct ridge and pseudofaults provide crucial information on timings of events. Combining these data with relative dating, and age estimates derived from spreading rate assumptions, helps build a sequence of events with approximate ages for ridge extinction, propagation and microplate formation.

Although sparse, magnetic anomaly picks near the extinct ridge can help approximate the timing of extinction. Cande et al.'s (2010) closest magnetic anomaly pick to the extinct ridge, and in fact one of only two from their study that is located in this spreading corridor within 1000 km from the ridge, is a single chron 22o (49.3 Ma) pick located ~150 km (spherical distance) from the western end of the ridge (Figs. 1c and 3). Based on the spreading rates of Cande and Patriat (2015), calculated for this part of the Southeast Indian Ridge (Fig. 1a – orange star), extinction likely occurred after chron 20o (43.4 Ma) in order for 150 km of crust to be produced. Their spreading rates predict that just under 150 km of crust was produced between chrons 22o and 20o. Two chron 21o (47.3 Ma) picks of Ségoufin et al. (2004) are located ~30 km north of the extinct ridge (Fig. 3). Based on Cande and Patriat's (2015) spreading rates, this would place the timing of extinction at chron 21y (45.7 Ma) at a minimum. It is difficult to place tight age constraints on extinction as it is uncertain whether spreading slowed at the dying ridge segment during its demise.

Similarly to the extinct ridge, the timing of ridge propagation and formation of the pseudofaults can be estimated using magnetic anomaly picks and spreading rate assumptions. When combined, these observations are found to be consistent with each other.

The age of the seafloor to the east of the pseudofaults, in the spreading corridor east of fracture zone E2 (Fig. 3), differs between the Antarctic and Indian plates. On the Antarctic Plate the seafloor formed at the time of chron 20o (43.4 Ma), whereas on the Indian Plate the chron 20o picks are located 230 km south, and therefore the seafloor is older. An age contrast strongly suggests that ridge propagation initiated from the site of a ridge offset rather than at a ridge tip, as in the instance of propagation from a ridge tip this age contrast should be the same on both plates. A model for an intratransform origin for ridge propagation was described in detail by Bird and Naar (1994) and has been proposed for many microplates in the Pacific, including the Bauer, Henry, Friday and Selkirk microplates (Eakins and Lonsdale, 2003; Tebbens et al., 1997; Tebbens and Cande, 1997; Blais et al., 2002). This is also seen to the west of Australia where ridge propagation from the large offset Wallaby-Zenith fracture zone appears to have initiated and then failed after ~100 km leaving two pseudofault traces. The nature of the age contrast across these spreading corridors is consistent with formation at a right-offset transform, which continued to present-day (Seton et al., 2012). Ridge propagation from a right offset transform indicates that propagation initiated at a time older than chron 20o, and younger than the time of formation of the crust to the east of the pseudofault on the Indian Plate. Considering that ~200 km of Indian Plate crust was produced between chrons 20o and chron 23.2o (47.3–51.8 Ma) (Cande and Patriat, 2015) this suggests ridge

propagation and pseudofault formation initiated after chron 23.2o (51.8 Ma).

In support of ridge propagation after chron 23.2o (51.8 Ma) is the observation that the pseudofault on the Antarctic Plate cuts seafloor that is chron 22o in age (49.3 Ma) (Fig. 3). Magnetic anomaly picks from both Cande et al. (2010) and Ségoufin et al. (2004) date seafloor in this region, which strengthens the observation. Propagation must therefore have occurred after this time.

Two chron 21o magnetic anomaly picks of Ségoufin et al. (2004) are located along strike and adjacent to the pseudofault (within 10 km) and may date the youngest seafloor formed at the new spreading centre. These ages are consistent with age estimates derived using the spreading rates of Cande and Patriat (2015). At the western end of the pseudofaults ~170 km of crust was produced on each flank of the new spreading ridge by the time of chron 18.2o (40.1 Ma), based on the isochron that we constructed using the magnetic anomaly picks of Cande et al. (2010) (trace of the Antarctic–Indian mid-ocean ridge in Fig. 3). At the eastern end of the pseudofaults closer to ~200 km of crust was produced on each flank. Based on spreading rate calculations for this portion of the ridge, propagation initiated around chron 21o (47.3 Ma) and was completed before the end of chron 21 (45.7 Ma), and therefore was likely completed in less than 2 Myr at a rate of c. 200 mm/yr. Considering that the full spreading rate at the Antarctic–Indian ridge between c23.2o and c20o ranged from ~110 to 75 mm/yr, this propagation rate is consistent with observations from intermediate-fast spreading ridges that ridge propagation can occur at rates of 50–150% of the full spreading rate at the ridge (Phipps Morgan and Sandwell, 1994).

In summary, a variety of age observations support rapid ridge propagation during chron 21. Ridge extinction is more difficult to constrain, but must have occurred after chron 21. The demise of spreading at the ridge may even have continued until after chron 20. Estimating the ages of these events is made difficult by the possibility of a period of slow spreading immediately prior to ridge death and immediately following the initiation of spreading at the new ridge.

5. Microplate formation in the eastern Indian Ocean

Seafloor tectonic fabric features, that are well-defined in recent VGG data (Sandwell et al., 2014), record a mid Eocene reorganization at the Southeast Indian Ridge to the west of the Ninetyeast Ridge, involving a southward ridge jump and formation of an oceanic microplate. We refer to this microplate as the Mammerickx Microplate, after Dr Jacqueline Mammerickx, a pioneer in seafloor mapping, in particular the mapping of microplates in the Pacific. Formation of the Mammerickx Microplate involved dual-spreading, including rotation of the dying ridge axis, and the formation of seafloor fabric features that are observed in the Pacific Ocean at the sites of well-studied microplates. The sequence of events associated with the reorganization is depicted in Fig. 6 and is constrained by magnetic anomalies (Cande et al., 2010; Ségoufin et al., 2004), relative age dating, and seafloor age estimates from the seafloor spreading data of Cande and Patriat (2015).

Westward ridge propagation from a developing right-offset transform fault initiated at approximately chron 21o (47.3 Ma) resulting in a southward ridge relocation. Propagation was rapid, c. 200 mm/yr, and was likely completed by the end of chron 21 (45.7 Ma). Spreading at the dying ridge likely ceased some time during or after chron 20 (43.4–42.3 Ma). During its demise the ridge grew southward and rotated clockwise, which in turn caused a counterclockwise rotation of existing seafloor fabric, such as abyssal hills to the south. This reorganization was not only associ-

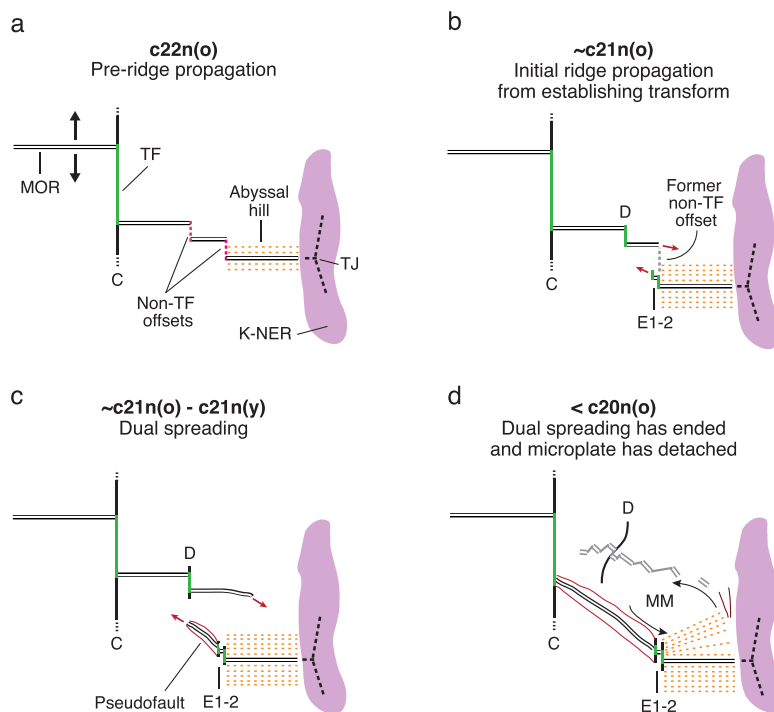


Fig. 6. Schematic reconstruction of the formation of the Mammerickx Microplate (MM). (a) Chron 22n(o) time (49.3 Ma) precedes microplate formation. At this time there is ~north-south directed spreading between the Indian and Antarctic plates, and to the east of fracture zone C the Indian-Antarctic ridge likely comprised non-transform offsets. (b) At approximately chron 21n(o) time (47.3 Ma) a reorganization at the Indian-Antarctic ridge initiates involving ridge propagation from a non-transform offset and the establishment of three transform faults at the ridge (fracture zones D, E1 and E2). (c) Dual-spreading at the newly establishing southerly ridge and the pre-existing northerly ridge occurs for a short period, approximately throughout chron 21n time (47.3–45.7 Ma). During formation of the Mammerickx Microplate the pre-existing northerly ridge lengthens in an easterly and southerly direction and curves inwards towards the microplate core leaving behind counterclockwise rotated abyssal hills. Rotation of the ridge is also reflected in the curvature of fracture zone D. (d) Dual-spreading has likely ceased and the microplate has detached after chron 20n(o) time (43.4 Ma). Volcanism associated with the Kerguelen Plateau (K) and Ninetyeast Ridge (NER), attributed to the Kerguelen Plume, is shown in purple. Transform (TF) offsets are green lines, and non-transform offsets are dashed magenta lines. The extinct northerly ridge is gray in (d). See Fig. 3 for the locations of fracture zones C, D, E1 and E2. MOR, mid-ocean ridge; TJ, triple junction. (For interpretation of the references to color in this figure legend, the reader is referred to the web version of this article.)

ated with a ridge jump, but also the establishment of a right-offset transform fault to the west of the Ninetyeast Ridge that has persisted to present-day. Ridge propagation coincides with the rapid change in spreading azimuth at the Central and Southeast Indian ridges identified by Cande et al. (2010).

6. Discussion

Identification of a microplate in the Indian Ocean is spatially significant as until now microplate formation has almost entirely been restricted to the Pacific, specifically at the East Pacific Rise and Pacific-Antarctic Ridge. This suggests that at the time of Mammerickx Microplate formation, kinematic or geodynamic conditions at this part of the Indian-Antarctic ridge shared similarities with those that have frequently been present at eastern Pacific ridge systems, yet largely absent in the Atlantic and elsewhere in the Indian Ocean.

As summarized by Hey (2004) the stresses related to plate reorganizations, fast spreading and hotspot activity can trigger or promote ridge propagation and the formation of microplates. Additionally, episodic triple junction migration has been associated with ridge propagation and microplate formation in the eastern Pacific (Bird et al., 1999; Tebbens et al., 1997; Tebbens and Cande, 1997); specifically formation of the Hudson, Friday and Juan Fernandez microplates occurred during migration of the Pacific-Antarctic-Nazca/Farallon triple junction (Tebbens et al., 1997; Tebbens and Cande, 1997; Eakins, 2002). Each of these four drivers may have played a role in formation of the Mammerickx Microplate.

Ridge propagation at chron 21o time (47.3 Ma) coincides with proposed timings of India-Eurasia collision; a major plate bound-

ary shake-up. Additionally, half-spreading rates at the Indian-Antarctic ridge exceeded 50 mm/yr prior to ridge propagation (Cande and Patriat, 2015), this is similar to present-day spreading rates at the fast spreading East Pacific Rise of 50 to >70 mm/yr (DeMets et al., 2010) and Cenozoic rates that typically exceeded 70 mm/yr (Müller et al., 2008). Furthermore, it has been proposed that hotspots can influence ridge behaviour over distances of up to 1400 km (Ribe and Delattre, 1998), and based on three different absolute reference frames (O'Neill et al., 2005; Doubrovine et al., 2012) the microplate formed less than 1100 km from the Kerguelen Hotspot centre point (location from Whittaker et al., 2015), or less than 700 km from the hotspot assuming a 400 km plume radius (Montelli et al., 2004) (Table 1). Ridge propagation, to the west, was directed away from the hotspot as predicted by models of ridge propagation (Phipps Morgan and Parmentier, 1985) and as seen in the Pacific (Hey and Wilson, 1982). Finally, plate reconstructions for the eastern Indian Ocean at this time (e.g. Whittaker et al., 2013) model a triple junction east of the microplate, with the Southeast Indian Ridge (comprising the Indian-Antarctic and Australian-Antarctic ridges) connected to the Wharton Ridge (Indian-Australian ridge) via a transform along the Ninetyeast Ridge (e.g. Seton et al., 2012).

We consider that a plate reorganization in the Indian Ocean, that included a rapid slow down in spreading between India and Antarctica at chron 21o (Cande and Patriat, 2015), triggered microplate formation. Plate reorganizations can change the stress field of a plate and the coupling across free-slip boundaries, leading to tearing and rift propagation (Bird and Naar, 1994; Eakins, 2002). In the eastern Indian Ocean the chron 21o reorganization altered the configuration of the Antarctic-Indian spreading

Table 1
Approximate distance between the Kerguelen Hotspot and the initiation point of the pseudofaults.

Reference frame	Distance to hotspot centre point ^a (edge of 400 km plume radius ^b)
Fixed hotspot	1090 km (690 km)
O'Neill et al. (2005), moving hotspot	650 km (250 km)
Doubrovine et al. (2012), moving hotspot	820 km (420 km)

^a Hotspot location (69°E, 49°S) from Whittaker et al. (2015).

^b Choice of 400 km plume radius is from Montelli et al. (2004).

ridge. Tearing from a newly established transform lead to westward ridge propagation and ultimately formation of the Mammerickx Microplate. This shares similarities with the formation of the Hudson Microplate, which involved ridge propagation from the newly formed Raitt transform (Eakins, 2002).

We further suggest that high spreading rates and proximity to the Kerguelen Plume likely facilitated the microplate formation event that was triggered by the chron 21o reorganization. Fast spreading rates and hot asthenosphere from plume activity can lead to formation of weak and thin lithosphere that is less able to resist cracking and rift propagation (Hey et al., 1985; Naar and Hey, 1989; Bott, 1993), and therefore produce a tectonic scenario conducive to microplate formation. These conditions, however, were both present for tens of millions of years in this part of the Indian Ocean and therefore are not considered as 'triggers' for the event. Fast spreading rates, exceeding 50 mm/yr (half-rate), were present at the Indian–Antarctic ridge for >20 Myr prior to a rapid decrease at chron 21o time (47.3 Ma) (Cande and Patriat, 2015). A rapid increase in spreading rate at the Southeast Indian Ridge occurred at chron 31y (68 Ma), with a peak half-spreading rate of 90 mm/yr recorded between chrons 29o and 28y (66–63 Ma) (Cande and Patriat, 2015). There has been a hotspot influence at the ridge for even longer. Whittaker et al. (2013) showed that over at least a 65 Myr period from 108 to 43 Ma, the position of the Australian–Indian–Antarctic triple junction was influenced by the Kerguelen Plume; the ridge system remained close to the plume, within 500 km during the period, and as close as 100 km by 43 Ma, assuming hotspot fixity. The southerly jump of the Indian–Antarctic ridge, achieved through microplate formation, is consistent with the ridge system moving towards and remaining close to the hotspot.

Fast spreading and plume activity may also be responsible for a large region of distinctively undulate and chaotic seafloor north of the extinct ridge (Fig. 4). Fast spreading prior to microplate formation hampered the establishment of stable transform offsets at the Indian–Antarctic ridge, resulting in the back and forth migration of ridge offsets. According to Naar and Hey (1989) half-spreading rates exceeding 75 mm/yr prevent transform fault formation, however here spreading rates were slightly slower at times, exceeding 50 mm/yr. Therefore plume activity, which can influence ridge behaviour over distances of up to 1400 km (e.g. Ribe and Delattre, 1998), likely contributed to the formation of weaker lithosphere, which when coupled with fast spreading rates resulted in back and forth ridge propagation. We speculate that pulses of plume activity may be responsible for the undulating seafloor topography and seamount like structures in this region.

It is difficult to access whether triple junction migration played a role in Mammerickx Microplate formation, as the plate boundary between Australia and Antarctica, in the region of the Kerguelen Plateau and Broken Ridge, may not have been a discrete boundary prior to 43 Ma, rather it may have been a diffuse boundary or composed of short-lived boundaries (Whittaker et al., 2013). The model for triple junction migration proposed by Bird et al. (1999) and applied to microplate formation in the Pacific involved a system of three discrete and well-established plate boundaries, and it is uncertain whether it can be applied in the eastern Indian Ocean

at this time. Additionally, ridge propagation leading to microplate formation did not occur directly at the triple junction.

The timing of microplate formation in the eastern Indian Ocean at 47 Ma is temporally significant as this time, corresponding to chron 21o, has been proposed as the initial India–Eurasia collision time by a number of authors (see summary in Cande and Patriat, 2015). Although there is considerable spread in the published timings of the India–Eurasia collision, and debate over the number and nature of collision events, formation of the Mammerickx Microplate adds support for a collision at ~47 Ma, as the initial continental collision between India and Eurasia would be expected to lead to a significant change in the stress regime at the Indian–Antarctic ridge. This initial stage of continent–continent collision, likely the 'soft' collision stage (Gibbons et al., 2015), not only slowed spreading at the Indian–Antarctic ridge (Cande and Patriat, 2015), but it also altered ridge segmentation and initiated ridge propagation. The connection between the onset of mountain building in Tibet, the post-47 Ma slowdown of the Indian Plate and the subsequent reorganization of plate boundaries in the Indian Ocean, as proposed in Copley et al.'s (2010) analysis of Indian Plate driving forces, fits with our observation of microplate formation recording the onset of this set of events in the Indian Ocean. There is a coincidence in timing between the India–Eurasia collision and a number of plate boundary reorganization events in other ocean basins (Whittaker et al., 2007), as well as the formation of the bend in the Hawaiian–Emperor seamount chain. However, it is beyond the scope of this investigation to test geodynamic linkages between these widely distributed events.

7. Conclusions

Our analysis of a new satellite-derived global VGG dataset (Sandwell et al., 2014), with unprecedented resolution, has revealed an extinct Pacific-style microplate in the eastern Indian Ocean – the 'Mammerickx Microplate'. The Mammerickx Microplate is located west of the Ninetyeast Ridge (centred on ~21.5°S), formed at the Indian–Antarctic ridge during the Eocene and was captured by the Indian Plate. To our knowledge this is the first of its kind in the Indian Ocean. A variety of seafloor structures, identified from high-resolution satellite-derived VGG data, match those at well-studied microplates in the eastern Pacific (e.g. Bauer, Friday, Mathematician, Hudson and Selkirk). These structures include conjugate pseudofaults produced by propagation of the new ridge, an extinct ridge and rotated abyssal hill fabric, the latter of which is observed in the VGG and ship track multibeam bathymetry data (Sojourn Expedition Leg 4, R/V Melville, 1997). The observation that the microplate underwent counterclockwise rotation reflects that dual spreading occurred prior to ridge extinction at the northern pre-existing ridge. This indicates there was a brief period during which the motion of the microplate was independent to that of the neighboring Indian and Antarctic plates, likely due to drag from the adjacent plates (Schouten et al., 1993; Eakins, 2002).

We propose that the formation of the Mammerickx Microplate is linked with the initiation of the India–Eurasia collision, with ridge propagation triggered by the event. Magnetic anomaly picks, relative age dating, and age estimates using recently published spreading rates for the Indian–Antarctic ridge (Cande and Patriat, 2015) were used to constrain microplate formation to chron 21o (47.3 Ma), with the initiation of westward directed propagators at this time.

Plate motion changes during reorganization events, such as those related to tectonic collisions, have been linked with microplate formation in the Pacific (e.g. Tebbens et al., 1997; Tebbens and Cande, 1997). In the case of the Mammerickx Microplate, we suggest that westward ridge propagation from a newly

formed transform was triggered by the initiation of the India–Eurasia collision and resultant changes to the stress regime at the ridge. This microplate formation event was coincident with a well-defined slow down in seafloor spreading (Cande and Patriat, 2015). We further suggest that hotspot activity and fast spreading rates (preceding collision), that are associated with warm, thin and weak lithosphere, facilitated ridge propagation and microplate formation, yet were less likely to have acted as triggers as both were present for tens of millions of years leading up to formation. They are also responsible for the production of chaotic and undulate seafloor north of the microplate and west of the Ninetyeast Ridge, in which ‘W’ shaped propagating ridge traces are common. Our dating of part of the history of the India–Eurasia collision is novel, completely independent from previous conclusions drawn from continental geology and convergence rate calculations, and represents the most precise and unambiguous date for the onset of India–Eurasia collision.

Acknowledgements

K.J.M. and R.D.M. were supported by ARC Discovery Project DP130101946. The CryoSat-2 data were provided by the European Space Agency, and NASA/CNES provided data from the Jason-1 altimeter. This research was supported by the National Science Foundation (OCE-1128801), the Office of Naval Research (N00014-12-1-0111), the National Geospatial-Intelligence Agency (HM0177-13-1-0008) and ConocoPhillips. Version 23 of the global grids of gravity anomaly and VGG can be downloaded from the following ftp site ftp://topex.ucsd.edu/pub/global_grav_1min. All figures were produced using the *Generic Mapping Tools (GMT)* software (Wessel et al., 2013). The open-source plate reconstruction software *GPlates* (Boyden et al., 2011) was used to compute the distance from the Kerguelen Plume to the initiation point of ridge propagation using different absolute reference frames, and to produce the VGG raster reconstruction in Fig. 3. Magnetic anomaly picks were accessed from the compilation of Seton et al. (2014) from The Global Seafloor Fabric and Magnetic Lineation Data Base Project website (<http://www.soest.hawaii.edu/PT/GSFML/>). We thank the editor An Yin and two anonymous reviewers for their thoughtful and constructive comments that improved the manuscript.

Appendix A. Supplementary material

Supplementary data related to this article can be found online at <http://dx.doi.org/10.1016/j.epsl.2015.10.040>. These data include the Google map of the most important areas described in this article.

References

- Aitchison, J.C., Ali, J.R., Davis, A.M., 2007. When and where did India and Asia collide? *J. Geophys. Res.* 112, 1–19.
- Becker, J.J., Sandwell, D.T., Smith, W.H.F., Braud, J., Binder, B., Depner, J., Fabre, D., Factor, J., Ingalls, S., Kim, S.H., Ladner, R., Marks, K., Nelson, S., Pharaoh, A., Trimmer, R., Von Rosenberg, J., Wallace, G., Weatherall, P., 2009. Global bathymetry and elevation data at 30 arc seconds resolution: SRTM30_PLUS. *Mar. Geod.* 32, 355–371.
- Bird, R.T., Naar, D.F., 1994. Intratransform origins of mid-ocean ridge microplates. *Geology* 22, 987–990.
- Bird, R.T., Tebbens, S.F., Kleinrock, M.C., Naar, D.F., 1999. Episodic triple-junction migration by rift propagation and microplates. *Geology* 27, 911–914.
- Blais, A., Gente, P., Maia, M., Naar, D.F., 2002. A history of the Selkirk paleomicroplate. *Tectonophysics* 359, 157–169.
- Bott, M.H.P., 1993. Modelling the plate-driving mechanism. *J. Geol. Soc.* 150, 941–951.
- Bouilhol, P., Jagoutz, O., Hanchar, J.M., Dudas, F.O., 2013. Dating the India–Eurasia collision through arc magmatic records. *Earth Planet. Sci. Lett.* 366, 163–175.
- Boyden, J.A., Müller, R.D., Gurnis, M., Torsvik, T.H., Clark, J.A., Turner, M., Ivey-Law, H., Watson, R.J., Cannon, J.S., 2011. Next-generation plate-tectonic reconstructions using GPlates. In: Keller, G.R., Baru, C. (Eds.), *Geoinformatics: Cyberinfrastructure for the Solid Earth Sciences*. Cambridge University Press, Cambridge, pp. 95–114.
- Cande, S.C., Patriat, P., 2015. The anticorrelated velocities of Africa and India in the Late Cretaceous and early Cenozoic. *Geophys. J. Int.* 200, 227–243.
- Cande, S.C., Patriat, P., Dymant, J., 2010. Motion between the Indian, Antarctic and African plates in the early Cenozoic. *Geophys. J. Int.* 183, 127–149.
- Copley, A., Avouac, J.P., Royer, J.Y., 2010. India–Asia collision and the Cenozoic slow-down of the Indian plate: implications for the forces driving plate motions. *J. Geophys. Res., Solid Earth* (1978–2012) 115.
- De Alteriis, G., Gilg Capar, L., Olivet, J.L., 1998. Matching satellite derived gravity signatures and seismicity patterns along mid-ocean ridges. *Terra Nova* 10, 177–182.
- DeMets, C., Gordon, R.G., Argus, D.F., 2010. Geologically current plate motions. *Geophys. J. Int.* 181, 1–80.
- Dobrovine, P.V., Steinberger, B., Torsvik, T.H., 2012. Absolute plate motions in a reference frame defined by moving hot spots in the Pacific, Atlantic, and Indian oceans. *J. Geophys. Res.* 117.
- Eakins, B.W., 2002. Structure and Development of Oceanic Rifted Margins, *Earth Sciences*. University of California, San Diego.
- Eakins, B.W., Lonsdale, P.F., 2003. Structural patterns and tectonic history of the Bauer microplate, Eastern Tropical Pacific. *Mar. Geophys. Res.* 24, 171–205.
- Gahagan, L.M., Scotese, C.R., Royer, J.-Y., Sandwell, D.T., Winn, J.K., Tomlins, R.L., Ross, M.I., Newman, J.S., Müller, R.D., Mayes, C.L., 1988. Tectonic fabric map of the ocean basins from satellite altimetry data. *Tectonophysics* 155, 1–6, 11–26.
- Gibbons, A.D., Zahirovic, S., Müller, R.D., Whittaker, J.M., Yattheesh, V., 2015. A tectonic model reconciling evidence for the collisions between India, Eurasia and intra-oceanic arcs of the central-eastern Tethys. *Gondwana Res.* 28, 451–492.
- Hafkenscheid, E., Wortel, M.J.R., Spakman, W., 2006. Subduction history of the Tethyan region derived from seismic tomography and tectonic reconstructions. *J. Geophys. Res.* 111, B08401.
- Hey, R.N., 1977. A new class of “pseudofaults” and their bearing on plate tectonics: a propagating rift model. *Earth Planet. Sci. Lett.* 37, 321–325.
- Hey, R.N., 2004. Propagating rifts and microplates at mid-ocean ridges. In: Selley, R.C., Cocks, R., Plimer, I. (Eds.), *Encyclopedia of Geology*. Academic Press, London, pp. 396–405.
- Hey, R.N., Wilson, D.S., 1982. Propagating rift explanation for the tectonic evolution of the northeast Pacific – the pseudomovie. *Earth Planet. Sci. Lett.* 58, 167–184.
- Hey, R.N., Duennebieber, F.K., Morgan, W.J., 1980. Propagating rifts on midocean ridges. *J. Geophys. Res.* 85, 3647–3658.
- Hey, R.N., Naar, D.F., Kleinrock, M.C., Phipps Morgan, W.J., Morales, E., Schilling, J.G., 1985. Microplate tectonics along a superfast seafloor spreading system near Easter Island. *Nature* 317, 320–325.
- Hey, R.N., Menard, H.W., Atwater, T.M., Cares, D.W., 1988. Changes in direction of seafloor spreading revisited. *J. Geophys. Res.* 93, 2803–2811.
- Klootwijk, C.T., Gee, J.S., Peirce, J.W., Smith, G.M., McFadden, P.L., 1992. An early India–Asia contact: paleomagnetic constraints from Ninetyeast ridge, ODP Leg 121. *Geology* 20, 395–398.
- Krishna, K.S., Rao, D.G., Ramana, M.V., Subrahmanyam, V., Sarma, K.V.L.N.S., Pilipenko, A.I., Shcherbakov, V.S., Murthy, I.V.R., 1995. Tectonic model for the evolution of oceanic crust in the northeastern Indian Ocean from the Late Cretaceous to the Early Tertiary. *J. Geophys. Res.* 100, 20011–20024.
- Krishna, K.S., Abraham, H., Sager, W.W., Pringle, M.S., Frey, F., Gopala Rao, D., Levchenko, O.V., 2012. Tectonics of the Ninetyeast Ridge derived from spreading records in adjacent oceanic basins and age constraints of the ridge. *J. Geophys. Res.* 117, B04101.
- Lee, T.-Y., Lawver, L.A., 1995. Cenozoic plate reconstruction of Southeast Asia. *Tectonophysics* 251, 85–138.
- Livermore, R., Balanyá, J.C., Maldonado, A., Martínez, J.M., Rodríguez-Fernández, J., de Galdeano, C.S., Zaldivar, J.G., Jabaloy, A., Barnolas, A., Somoza, L., Hernández-Molina, J., Suriñach, E., Vissers, C., 2000. Autopsy on a dead spreading center: the Phoenix Ridge, Drake Passage, Antarctica. *Geology* 28, 607–610.
- MacDonald, K.C., Scheirer, D.S., Carbotte, S.M., 1991. Mid-ocean ridges: discontinuities, segments and giant cracks. *Science* 253, 986.
- Mammerickx, J., Klitgord, K.D., 1982. Northern East Pacific Rise: evolution from 25 m.y. B.P. to the present. *J. Geophys. Res.* 87, 6751–6759.
- Mammerickx, J., Naar, D.F., Tyce, R.L., 1988. The mathematician paleoplate. *J. Geophys. Res.* 93, 3025–3040.
- Matthews, K.J., Müller, R.D., Wessel, P., Whittaker, J.M., 2011. The tectonic fabric of the ocean basins. *J. Geophys. Res.* 116, B12109.
- Molnar, P., Tapponnier, P., 1975. Cenozoic tectonics of Asia: effects of a continental collision. *Science* 189, 419–426.
- Montelli, R., Nolet, G., Dahlen, F.A., Masters, G., Engdahl, E.R., Hung, S.H., 2004. Finite-frequency tomography reveals a variety of plumes in the mantle. *Science* 303, 338.
- Müller, R.D., Sdrolias, M., Gaina, C., Roest, W.R., 2008. Age, spreading rates, and spreading asymmetry of the world’s ocean crust. *Geochem. Geophys. Geosyst.* 9, Q04006.

- Naar, D.F., Hey, R.N., 1989. Speed limit for oceanic transform faults. *Geology* 17, 420–422.
- NOAA National Centers for Environmental Information (2004). Multibeam Bathymetry Database (MBBDB), Sojourn Expedition Leg 4, R/V Melville, 1997. NOAA National Centers for Environmental Information. <http://dx.doi.org/10.7289/V56T0JNC>. Accessed on 14 July 2015.
- O'Neill, C., Müller, D., Steinberger, B., 2005. On the uncertainties in hot spot reconstructions and the significance of moving hot spot reference frames. *Geochem. Geophys. Geosyst.* 6.
- Ogg, J.G., 2012. Geomagnetic polarity time scale. In: Gradstein, F.M., Ogg, J.G., Schmitz, M., Ogg, G. (Eds.), *The Geologic Time Scale 2012*. Elsevier, Oxford, UK, p. 1176.
- Patriat, P., Achache, J., 1984. India–Eurasia collision chronology has implications for crustal shortening and driving mechanism of plates. *Nature* 311, 615–621.
- Phipps Morgan, J., Parmentier, E.M., 1985. Causes and rate-limiting mechanisms of ridge propagation: a fracture mechanics model. *J. Geophys. Res.* 90, 8603–8612.
- Phipps Morgan, J., Sandwell, D.T., 1994. Systematics of ridge propagation south of 30 S. *Earth Planet. Sci. Lett.* 121, 245–258.
- Replumaz, A., Karason, H., van der Hilst, R.D., Besse, J., Tapponnier, P., 2004. 4-D evolution of SE Asia's mantle from geological reconstructions and seismic tomography. *Earth Planet. Sci. Lett.* 221, 103–115.
- Ribe, N.M., Delattre, W.L., 1998. The dynamics of plume–ridge interaction – III. The effects of ridge migration. *Geophys. J. Int.* 133, 511–518.
- Rowley, D.B., 1998. Minimum age of initiation of collision between India and Asia north of Everest based on the subsidence history of the Zhepure Mountain section. *J. Geol.* 106, 220–235.
- Sandwell, D.T., Smith, W.H.F., 2009. Global marine gravity from retracked Geosat and ERS-1 altimetry: ridge segmentation versus spreading rate. *J. Geophys. Res.* 114, B01411.
- Sandwell, D.T., Müller, R.D., Smith, W.H., Garcia, E., Francis, R., 2014. New global marine gravity model from CryoSat-2 and Jason-1 reveals buried tectonic structure. *Science* 346, 65–67.
- Schouten, H., Klitgord, K.D., Gallo, D.G., 1993. Edge-driven microplate kinematics. *J. Geophys. Res.* 98, 6689–6701.
- Searle, M.P., Windley, B.F., Coward, M.P., Cooper, D.J.W., Rex, A.J., Rex, D., Tingdong, L., Xuchang, X., Jan, M.Q., Thakur, V.C., Kumar, S., 1987. The closing of the Tethys and the tectonics of the Himalaya. *Geol. Soc. Am. Bull.* 98.
- Searle, R.C., Bird, R.T., Rusby, R.I., Naar, D.F., 1993. The development of two oceanic microplates: Easter and Juan Fernandez microplates, East Pacific Rise. *J. Geol. Soc.* 150, 965–976.
- Ségoufin, J., Munschy, P., Bouysse, P., Mendel, V., Grikurov, G., Leitchenkov, G., Subrahmanyam, C., Chand, S., Pubellier, S., Patriat, P., 2004. Map of the Indian Ocean (1:20 000 000), sheet 1: "Physiography", sheet 2: "Structural map". Commission for the Geological Map of the World, Paris.
- Seton, M., Müller, R.D., Zahirovic, S., Gaina, C., Torsvik, T.H., Shephard, G., Talsma, A., Gurnis, M., Turner, M., Maus, S., Chandler, M., 2012. Global continental and ocean basin reconstructions since 200 Ma. *Earth-Sci. Rev.* 113, 212–270.
- Seton, M., Whittaker, J.M., Wessel, P., Müller, R.D., DeMets, C., Merkouriev, S., Cande, S., Gaina, C., Eagles, G., Granot, R., 2014. Community infrastructure and repository for marine magnetic identifications. *Geochem. Geophys. Geosyst.* 15, 1629–1641.
- Small, C., 1995. Observations of ridge–hotspot interactions in the Southern Ocean. *J. Geophys. Res.* 100, 17931–17946.
- Tebbens, S.F., Cande, S.C., 1997. Southeast Pacific tectonic evolution from Early Oligocene to present. *J. Geophys. Res.* 102, 12061–12084.
- Tebbens, S.F., Cande, S.C., Kovacs, L., Parra, J.C., LaBrecque, J.L., Vergara, H., 1997. The Chile ridge: a tectonic framework. *J. Geophys. Res.* 102, 12035–12059.
- van der Voo, R., Spakman, W., Bijwaard, H., 1999. Tethyan subducted slabs under India. *Earth Planet. Sci. Lett.* 171, 7–20.
- van Hinsbergen, D.J.J., Lippert, P.C., Dupont-Nivet, G., McQuarrie, N., Doubrovine, P.V., Spakman, W., Torsvik, T.H., 2012. Greater India Basin hypothesis and a two-stage Cenozoic collision between India and Asia. *Proc. Natl. Acad. Sci. USA* 109, 7659–7664.
- Wessel, P., Smith, W.H.F., Scharroo, R., Luis, J., Wobbe, F., 2013. Generic mapping tools: improved version released. *Eos, Trans. Am. Geophys. Union* 94, 409–410.
- Whittaker, J.M., Müller, R.D., Leitchenkov, G., Stagg, H., Sdrolias, M., Gaina, C., Goncecharov, A., 2007. Major Australian–Antarctic plate reorganization at Hawaiian–Emperor bend time. *Science* 318, 83–86.
- Whittaker, J.M., Williams, S.E., Müller, R.D., 2013. Revised tectonic evolution of the Eastern Indian Ocean. *Geochem. Geophys. Geosyst.* 14, 1891–1909.
- Whittaker, J.M., Afonso, J.C., Masteron, S., Müller, R.D., Wessel, P., Williams, S.E., Seton, M., 2015. Long-term interaction between mid-ocean ridges and mantle plumes. *Nat. Geosci.* 8, 479–483.
- Zahirovic, S., Müller, R.D., Seton, M., Flament, N., Gurnis, M., Whittaker, J., 2012. Insights on the kinematics of the India–Eurasia collision from global geodynamic models. *Geochem. Geophys. Geosyst.* 13.